Pharm Res (2014) 31:1575–1587
DOI 10.1007/s11095-013-1263-5

RESEARCH PAPER

Significance of Unfolding Thermodynamics for Predicting Aggregation Kinetics: A Case Study on High Concentration Solutions of a Multi-Domain Protein

Atul Saluja • Vikram Sadineni • Amol Mungikar • Vishal Nashine • Andrew Kroetsch • Charles Dahlheim • Venkatramana M. Rao

Received: 26 July 2013 / Accepted: 9 December 2013 / Published online: 8 January 2014

ABSTRACT

Purpose To enable aggregation rate prediction over a broad temperature range for complex multi-domain proteins at high concentrations.

Methods Thermal unfolding, non-isothermal kinetics and storage stability studies were conducted on a model multi-domain protein (MDP) at moderate to high concentrations (25–125 mg/mL) over a broad temperature range (4–40°C).

Results Storage stability studies indicated the aggregation of MDP in solution to be a second order process. Application of Arrhenius kinetics to accelerated stability data resulted in underestimation of the aggregation rate under refrigerated conditions. Additional studies undertaken to understand the mechanism of the aggregation process highlighted the association of the monomer (or the aggregation competent species) to be the rate-limiting step for aggregation over the temperature range studied. Thermal unfolding studies in the presence of urea were used to calculate the heat capacity change upon unfolding ($\Delta c_{p,un}$). The resulting value of $\Delta c_{p,un}$ when used in the extended Lumry-Eyring model resulted in a more accurate and a conservative estimate of the aggregation rate under refrigerated condition. Some complicating factors for the aggregation rate prediction for multi-domain proteins at high concentration are discussed.

Conclusions The work highlights (i) the significance of incorporating unfolding thermodynamics in protein aggregation rate prediction, (ii) the advantages and challenges associated with the use of the extended Lumry-Eyring (ELE) model for rate prediction and (iii) the utility of using the Arrhenius and the ELE models in tandem during product development.

A. Saluja • V. Sadineni • A. Mungikar • V. Nashine • A. Kroetsch • C. Dahlheim • V. M. Rao (✉)
Drug Product Science and Technology, Bristol-Myers Squibb Co.
One Squibb Drive, New Brunswick, New Jersey 08903, USA
e-mail: venkatramana.rao@bms.com

KEY WORDS arrhenius kinetics · extended lumry-eyring model · protein aggregation · protein formulation · physical stability · protein unfolding · shelf-life · thermodynamics

INTRODUCTION

Aggregates, a major degradation product of monomeric proteins, can potentially impact the safety, efficacy and quality of a biopharmaceutical product (1–4). Numerous reports in literature cite the direct or indirect involvement of aggregates in inducing an immune response against the degraded product in animal models (5,6). Other reports highlight the role of neutralizing antibodies produced in response to the aggregates or non-native monomers in undermining the efficacy of the product (7–9). The possible influence of aggregated species on safety and efficacy in humans per se, although not extensively documented, is very well appreciated (10,11). Given the deleterious effects of aggregates in protein products, characterization and control of the aggregation phenomenon has been and continues to be one of the more significant aspects of protein product development.

Knowledge of the aggregation rates under refrigerated conditions is one of the key variables, besides chemical degradation rates, which impacts the development of product specifications (12,13). However, the relatively slower rates of reaction under refrigerated conditions and the time required to generate significant levels of aggregates makes the direct determination of aggregation rate under these conditions an unrealistic and impractical exercise during development. Consequently, predictive models aimed at estimating aggregation rates under refrigerated conditions from accelerated stability data can prove indispensible in improving the efficiency of the formulation development process. Additionally, it is not uncommon to encounter solution conditions which

impact different attributes of a product with opposing effects. For example, salts are known to decrease solution viscosity of certain protein solutions, often a desired effect, while simultaneously increasing the rate of aggregation (14,15), an undesirable effect. In instances like this, it is not simply enough to compare multiple solution conditions on a qualitative basis. Quantitative estimate of the product attributes under refrigerated storage conditions is desired.

A generalized mechanism proposed for non-native aggregation proceeds via the first order reversible formation of an intermediate or aggregation competent species (M*) from the native protein (M) and its subsequent irreversible assembly in a higher order process to form aggregates (M*n) (16,17) . This is a rather simplistic representation of the overall aggregation process and additional steps including the generation of multiple conformational states as well as multiple pathways for growth and polymerization of the dimers into oligomers may be involved (18). However, it offers a good starting point for understanding the overall process. The Arrhenius model (Eq. 1), historically used for degradation rate prediction of small molecules, offers a simplistic approach to predicting aggregation rates in protein solution.

$$\ln k_{1,T}^{app} = \ln k_{1,T_{ref}}^{app} - \frac{E_a}{R}\left(\frac{1}{T} - \frac{1}{T_{ref}}\right) \quad (1)$$

In Eq. 1, k_1^{app} is the apparent degradation rate constant, T is the long-term storage temperature, T_{ref} is a reference accelerated condition temperature, E_a is the activation energy and R is the gas constant. The term k_1^{app} is a composite of (i) the configurational equilibrium between M and M* i.e. the unfolding-refolding rates and the intrinsic rate of assembly of M* to M*n (19). It is fairly well understood that the rates of degradation of proteins may not exhibit an Arrhenius behavior when extrapolated over a relatively broad range of temperature. However, researchers employ the Arrhenius approximation to protein solutions in an attempt to derive a more conservative, rather than accurate, estimate of the degradation rate (overestimation of rate) and subsequently the product shelf-life (underestimation of shelf-life). Recent work by Chris Roberts *et al.* (19) sheds light on the inadequacy of the Arrhenius approach in the context of protein solutions. Contrary to the assumption, authors have highlighted case studies in which storage shelf-life can be overestimated if one employs the Arrhenius extrapolation for aggregation prediction in protein solutions.

When applied to proteins in theory, the Arrhenius model primarily accounts for the energy required to generate the aggregation-competent species (activation energy), its association or assembly to generate the oligomeric species and its growth over time (20) without much regard to the process of protein unfolding and the kinetics of it. Recent literature offers more realistic models and data treatments for predicting aggregation in protein solutions exhibiting non-Arrhenius behavior (21–24). Although a number of analytical treatments exist, none is universally applicable. One set of suggested models, classified as the extended Lumry-Eyring (ELE) models (19,24–26) takes into account the contributions of both (i) the thermodynamics of the reversible conformational change i.e. the unfolding process and (ii) the irreversible molecular association or the assembly process in predicting the rate of protein aggregation and thus appears to be a natural extension of the Arrhenius model. The temperature dependence of the aggregation rate can then be represented by Eq. 2 (24).

$$\ln k_{1,T}^{app} = \ln k_{1,T_{ref}}^{app} - \frac{E_a}{R}\left(\frac{1}{T} - \frac{1}{T_{ref}}\right) - \frac{\Delta c_{p,un}}{R}\left(1 - \frac{T_{ref}}{T} + \ln\frac{T_{ref}}{T}\right) \quad (2)$$

In Eq. 2, $\Delta c_{p,un}$ is the heat capacity change from the folded to the aggregation-competent partially or fully unfolded form of the monomer. The above expression highlights the need to better characterize the unfolding behavior of the protein in order to predict aggregation rates for non-Arrhenius systems. The authors (24) have shown the validity of the ELE model in predicting aggregation rates for recombinant bovine granulocyte-colony stimulating factor (bG-CSF); a single domain protein exhibiting a reversible two-state transition in which the aggregation-competent form of the monomer exists in solution for a considerable time (i.e. it can be isolated and characterized via biophysical techniques). However, a majority of the protein molecules under development today are more complex in their structure and behavior. For example, monoclonal antibodies and various kinds of fusion proteins have multiple domains that do not unfold in a cooperative manner and thus do not follow a simple two-state unfolding model. Predicting aggregation rates for these multi-domain molecules in solution presents a unique set of challenges.

Here we present a case study aimed at understanding and predicting the aggregation behavior of a multi-domain Fc-fusion protein (MDP) that (i) exhibits non-Arrhenius kinetics and (ii) a non-two-state transition process in solution. We characterized the aggregation of MDP via temperature (isothermal and non-isothermal) and concentration studies and compared the results of the Arrhenius and ELE model (24) for predicting aggregation rate of the protein in solution. The work presented in this manuscript attempts to highlight (i) the practical significance of incorporating unfolding thermodynamics in predicting protein aggregation rates and the pitfalls of not doing so (e.g. for prediction of shelf-life), (ii) the advantages as well as the challenges associated with the use of the ELE model for predicting aggregation rates of multi-

domain therapeutic proteins and (iii) the significance of using the ELE and the Arrhenius approach in tandem to bracket the aggregation rates under refrigerated storage conditions for a more robust product development exercise.

MATERIALS AND METHODS

Materials

The model protein for this work, MDP, was obtained from the drug product development group at BMS at a concentration of about 125 mg/mL in a pH 7.2 buffer. Dilution of the initial bulk, if needed, was done using the formulation buffer (10 mM sodium phosphate, 500 mM sucrose, 0.8% Polaxamer-188, pH 7.2). All chemicals used in the preparation of buffers and other solutions were of analytical grade or better.

Methods

Storage Stability

Accelerated stability studies were conducted on 2 mL aliquots in 5-mL type-1 borosilicate glass vials. Solutions of MDP at 25, 75 and 125 mg/mL in formulation buffer were studied at 25°C, 30°C, 35°C, and 40°C. Vials were filled aseptically, stoppered, sealed and stored in an upright position at specified temperatures. Sample vials were pulled at predetermined time-points and analyzed via size-exclusion chromatography. Long-term storage studies were conducted on multiple batches of MDP at 125 mg/mL in glass syringes placed at 2–8°C over a period of 1–2 years.

Protein Concentration

Protein concentration was measured using an Agilent 8453 UV–Vis spectrophotometer (Agilent Technologies, Santa Clara, CA). Absorbance was monitored at 280 nm and concentration calculated using an extinction coefficient of 1.01 mL/mg/cm.

Size-Exclusion Chromatography (SEC)

A Waters Alliance 2695 separation module equipped with a Waters W2487 dual channel UV/Vis detector (Waters Corporation, Milford, MA) was used for SEC analysis. A TSKgel 5 μ 3000SWxL size-exclusion column along with a TSKgel 7 μ 3000SWxL guard column (Tosoh Bioscience, King of Prussia, PA) were used to quantify the amount of monomer remaining in each sample. The auto-sampler module was maintained at 4°C while the column was operated at room temperature. A solution of 0.2 M potassium phosphate with 0.9% (w/v) sodium chloride at pH 6.8 was used as the mobile phase. Protein load on the column was kept between 200 and 250 μg (depending on the starting concentration) and the samples were analyzed without any additional dilution. A flow-rate of 1 mL/min was used with a run time of 20 min. Detection was carried out at 280 nm.

Unfolding-Refolding Kinetics

Unfolding and refolding studies were monitored at 25°C through intrinsic fluorescence studies using a Varian Cary Eclipse Fluorescence Spectrophotometer (Agilent Technologies, Santa Clara, CA). Excitation was conducted at 280 nm and emission was monitored at 355 nm. For unfolding experiments, a series of solutions containing guanidinium hydrochloride (Gd.HCl) from 1.35 M to1.75 M and 1 mg/mL protein in formulation buffer were prepared by mixing stock solutions of Gd.HCl (4 M in formulation buffer) and protein (125 mg/mL). The choice of Gd.HCl concentrations for the study was based on instrument sensitivity at the lower end and instrument's detection limit at the upper end. Increase in fluorescence intensity over the initial value ($y_{0,u}$) was monitored until a plateau (y_{max}) was obtained. A slit width of 5 nm was used for both excitation and emission. For refolding studies, protein samples at 2 mg/mL were prepared with Gd.HCl at twice the concentration of that used for unfolding studies (2.7–3.5 M) and left to equilibrate overnight at room temperature. Refolding was initiated by diluting the samples one-to-one with the formulation buffer. Slit widths used were 2.5 nm for excitation and 5 nm for excitation. Decrease in fluorescence intensity from the initial value ($y_{0,f}$) was monitored until no further decrease could be observed (y_{min}). All samples were analyzed in triplicate and data averaged. Unfolding (k_u) and refolding (k_f) rates were determined by fitting (using Prism™ by GraphPad Software, Inc., La Jolla, CA) Eq. 3 (unfolding) and Eq. 4 (refolding) to fluorescence data.

$$y = y_{0,u} + \left(y_{\max} - y_{0,u}\right)\left(1 - e^{-k_u t}\right) \tag{3}$$

$$y = y_{\min} + \left(y_{0,f} - y_{\min}\right)e^{-k_f t} \tag{4}$$

Thermal Scanning: Intrinsic Fluorescence (TSIF)

Urea induced unfolding studies were undertaken to characterize the unfolding process and to determine the $\Delta c_{p,un}$ for MDP in solution. Stock solutions of urea (8 M) in the formulation buffer and protein (125 mg/mL) were mixed to prepare a series of solutions with urea at concentrations between 0 and

2.5 M and protein concentration of 1 mg/mL. Solutions were heated at 1°C/min and intrinsic fluorescence intensity was monitored. Limited studies were also conducted at 0.5°C/min to evaluate the effect of scan rate on unfolding transition. Heat capacity change for MDP was calculated using the method proposed by Bolen *et al.* (27,28). Equation 5 was fitted to the thermal unfolding data generated in presence of urea to determine the unfolding enthalpy change (ΔH_m) at the melting temperature (T_m)

$$I = \frac{(In_N + m_N T) + (In_U + m_U T) * \exp[(\Delta H_m/RT) * ((T-T_m)/T_m)]}{1 + \exp[(\Delta H_m/RT) * ((T-T_m)/T_m)]} \quad (5)$$

In Eq. 5, I is the signal intensity, In_N is the intercept of the pre-transition native form of the protein, m_N is the slope of the native monomer *vs*. temp plot (pre-transitional baseline), In_U is the intercept of the unfolded aggregation-competent form, m_U is the slope of the unfolded aggregation-competent form *vs*. temp plot (post-transitional baseline).

Thermal Scanning: Extrinsic Fluorescence (TSEF)

Extrinsic fluorescence studies were conducted to evaluate the unfolding behavior of MDP at high concentration (125 mg/mL). Sypro orange dye was used as an *in-situ* extrinsic fluorescence probe for protein unfolding. A step-wise thermal ramp from 25 to 95°C was achieved using the CFX96 Real-Time PCR Detection System (Bio-Rad, Hercules, CA). A series of temperature steps (0.7°C increment) and time holds (15 s hold; 13.8 s read times) produced an effective scan rate of 1.5°C/min. A 1 μL aliquot of 200X dye stock solution (the absolute dye concentration is not published by the manufacturer) was spiked into each well containing 40 μL of 125 mg/mL MDP resulting in a final dye concentration of 5X. Samples were excited from 515 to 535 nm and emission was monitored from 560 to 580 nm.

Non-isothermal Kinetics

Non-isothermal-kinetic studies were conducted to understand the correlation between unfolding and aggregation behavior of MDP. For this purpose, 1.5 mL each of MDP solutions at 1.25 mg/mL, 12.5 mg/mL and 125 mg/mL in formulation buffer were heated at 1.5°C/min on the Varian Cary Eclipse Fluorescence Spectrophotometer. A Teflon stir bar was used to ensure content and thermal homogeneity throughout the run. Aliquots (80 μL) were collected during the course of the thermal ramp at predetermined temperatures, quenched on an ice bath for a minimum of 5 min and were analyzed via SEC. The monomer fraction remaining in solution was plotted as a function of solution temperature for each of the three MDP concentrations studied.

RESULTS

Long-Term Aggregation

Aggregation rates for MDP (~125 mg/mL) under refrigerated conditions (2–8°C) were determined following incubation of samples for a period of up to 2 years. Size-exclusion chromatography (SEC) analysis of MDP showed the formation of dimers, which was confirmed through light scattering studies (data not shown), as the predominant high-molecular weight (HMW) species (Fig. 1a). Detectable levels of any low-molecular weight (LMW) species were not observed during the course of the study. The aggregation rate was consistent with a second-order process (see Discussion section). The real-time rate constant was determined by plotting the inverse of the monomer concentration, 1/[M] *vs*. time (Fig. 1b) as per Eq. 6. Decent fits ($R^2 > 0.97$) to the data were obtained for the three lots studied.

$$\frac{1}{[M]} = \frac{1}{[M_0]} + k_1^{app} * t \quad (6)$$

Stability data was gathered for three different lots of MDP and an average aggregation (or monomer loss) rate of $8 \pm 1 \times 10^{-8}$ mL/(mg.day) was calculated. The calculated rate constant equated to a long-term rate of monomer loss, in the form of aggregates, of 0.44 ± 0.6%/year.

Unfolding-Refolding Equilibrium

In order to evaluate the unfolding-refolding kinetics for MDP, Gd.HCl induced unfolding studies were conducted at 1.0 mg/mL protein concentration (Fig. 2a). Representative unfolding and refolding curves are shown for 1.75 M Gd.HCl in Fig. 2a. Subsequently, Eqs. 3 and 4 were fitted to the fluorescence data to determine the unfolding and refolding rate constants as a function of Gd.HCl concentration (Fig. 2b). The refolding rate constants exhibited a linear dependence on the denaturant concentration whereas the unfolding rate constants exhibited a near-exponential behavior. Although we did not investigate the reason for this behavior, multiple reasons have been proposed in the literature for such a behavior including change in the ground state of the native monomer with increasing concentration of the denaturant and interactions between sequential transitions i.e. multiple domains of the protein (29,30). The refolding, upon sudden dilution of the denaturant, may still be cooperative

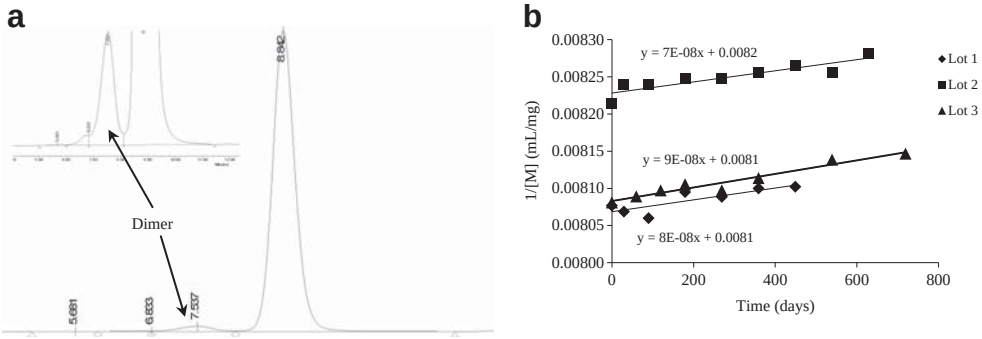

Fig. 1 Long-term aggregation kinetics. (**a**) Representative SEC chromatogram for MDP with inset showing the aggregated species. (**b**) Change in monomer concentration over time for three different lots of MDP when stored at 2–8°C. The monomer concentrations is plotted as 1/[M] *vs*. time.

and thus exhibited a linear dependence on denaturant concentration. Regardless, the results did not interfere with the determination of approximate unfolding and refolding rate constants and half-lives in the absence of denaturant. The intercepts, i.e. rate constants in the absence of denaturant, for the unfolding and refolding plots were determined to be 0.11/min and 6.51/min, respectively resulting in an unfolding half-life of 6.8 mins and a refolding half-life of 0.1 min. It may also be noted that the denaturant concentration for this experiment was chosen (i) to ensure a measurable unfolding/refolding rate (at the lower end of denaturant concentration) as well as to stay within the upper bounds of instrument's detection limit (at the upper end of denaturant concentration) and (ii) to limit the possibility of multiple domains unfolding/refolding simultaneously (as much as practically possible) or in quick succession, relative the timescale of the experiment and complicating the overall rate determination. Preliminary experiments exhibited a significantly poor signal at denaturant concentrations below 1 M Gd.HCl. Given the narrow range of the denaturant concentration studied and the non-linear dependence of unfolding rate constant with denaturant concentration, it should be noted that the calculated half-lives are only approximate. Additionally, it was not immediately clear as to which single transition, if at all, was contributing to the overall unfolding-refolding kinetics studied in this experiment. It is possible that a diverse population of partially to fully unfolded states of MDP may have co-existed at a given denaturant concentration.

Accelerated Storage Ability

Accelerated storage stability study was conducted by incubating 25 mg/mL, 75 mg/mL and 125 mg/mL MDP solutions at 25°C, 30°C, 35°C and 40°C over a period of 12 days (Fig. 3a-d). Since the intent was to limit the extent of the reaction to the formation of a small percentage of aggregates, consistent with what is observed in protein products over their entire shelf-life (usually <5%), we analyzed samples stored over a relatively shorter period of 12 days. Additional analysis was conducted wherein MDP solutions incubated at 40°C were diluted and the level of aggregates was compared to that of the undiluted samples. No significant difference was noted between the measured aggregate fractions for the diluted and undiluted samples confirming that the aggregates present in solution were not reversing to form monomers during the course of the SEC assay. All samples exhibited dimers and higher order aggregates with the extent of higher order aggregates increasing with temperatures as expected (Fig. 3e). For samples stored at 40°C, a significantly higher amount of monomer loss was noted during the course of the study compared to the other temperatures. Good fits of Eq. 6 to the data at 25°C, 30°C and 35°C were obtained ($R^2 > 0.99$). However, the quality of the fit and the changing intercept value for data at 40°C ($R^2 = 0.97$) indicated that the mechanism for the monomer loss might be changing at higher temperature and/or at higher extent of the reaction. Regardless, approximate second order initial rate constants

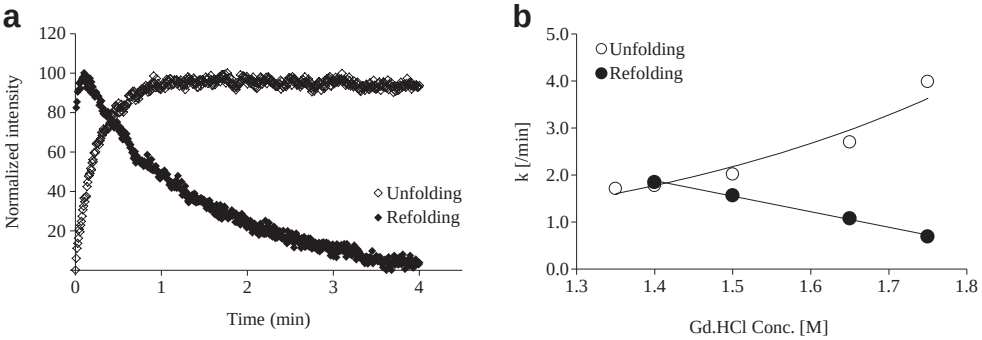

Fig. 2 Unfolding-refolding kinetics. (**a**) Fluorescence intensity for 1.0 mg/mL MDP at 25°C as a function of time in the presence of 1.75 M guanidinium hydrochloride. (**b**) Unfolding and refolding rates as determined by fitting Eqs. 3 and 4 to the unfolding-refolding fluorescence data.

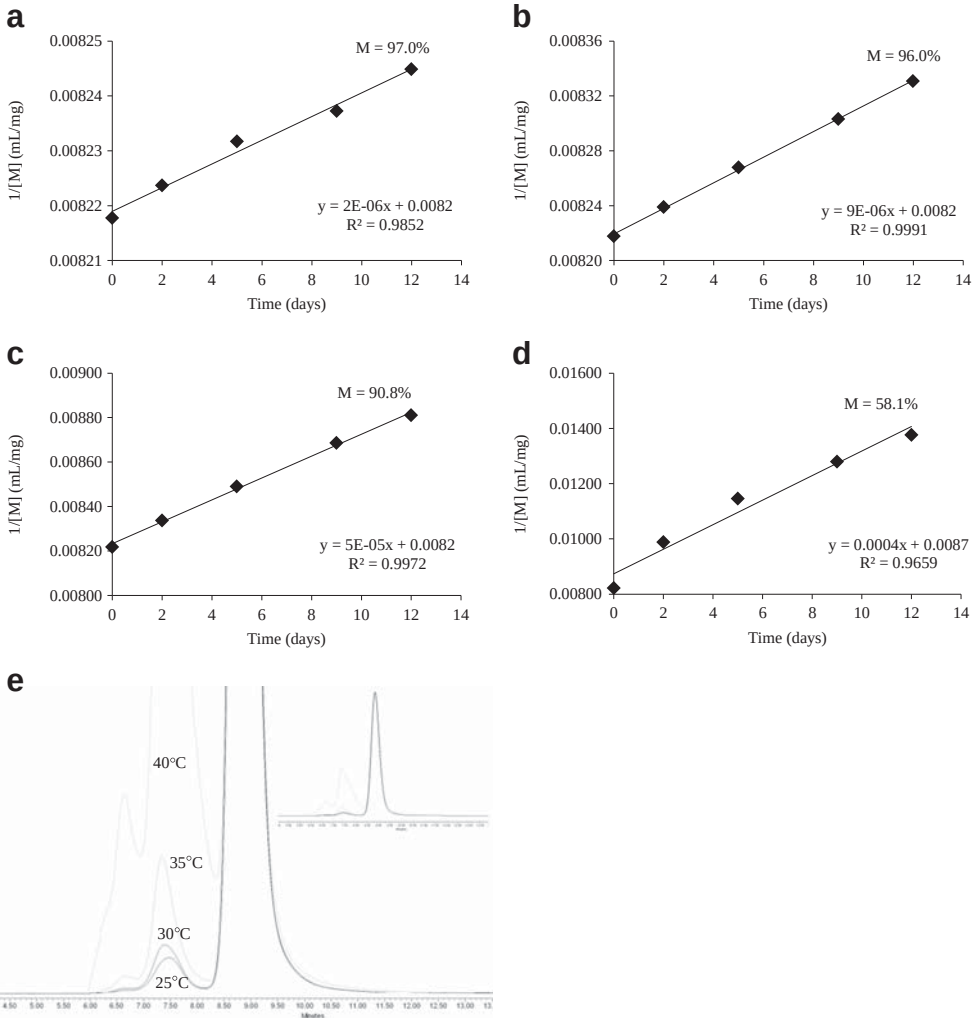

Fig. 3 Accelerated storage stability. Change in monomer concentration (plotted as 1/[M]) with time for 125 mg/mL MDP when stored at (**a**) 25°C, (**b**) 30°C, (**c**) 35°C and (**d**) 40°C. The slope represents the second order rate constant, k_1^{app}. The number in each plot at the last time-point indicates the percent monomer remaining in solution. (**e**) Normalized SEC chromatograms for 125 mg/mL MDP showing the increase in aggregated species with temperature following 12 days of storage; inset shows the full view of the SEC chromatograms.

could be calculated from the slopes of the four plots. For all the temperatures studied, SEC recovery (based on mass balance) was observed to be ~100%, within the error of the measurement, indicating insignificant loss of protein in the form of insoluble aggregates on the column matrix during analysis. Detectable levels of any low-molecular weight (LMW) species were not observed during the course of the study (Fig. 3e inset).

Conformational Transitions of MDP

To characterize the unfolding behavior of MDP in solution, intrinsic fluorescence scanning study was conducted for 1.0 mg/mL MDP in presence of increasing concentrations of urea. Since the intent of the experiment was to study the complete transition from native to the unfolded state and to determine $\Delta c_{p,un}$ of the aggregation-relevant transition, it was critical for MDP to maintain its native conformation in the presence of the denaturant at the lowest temperature i.e. 20°C prior to the start of the temperature ramp. Preliminary studies with roughly equimolar amounts of Gd.HCl appeared to indicate interference from protein unfolding during sample preparation and prior to the start of the thermal treatment. Consequently, Gd.HCl could not be used for this particular study. During the course of the thermal scan, two distinct transitions were noted. The first with a T_{onset} (temperature for the onset of unfolding transition) of ~50°C and the second one at ~80°C in absence of urea (Fig. 4). No significant difference of the scan rate was observed on the T_{onset} (data not shown). With addition of urea, T_{onset} for the two transitions decreased indicating reduced conformational stability in the presence of urea. At the start of the thermal ramp, the fluorescence intensity of MDP in absence and presence of urea was similar (between 124 and 132 a.u.) indicating a native or near-native conformation in all the solutions at 20°C. During thermal ramp, the linear decrease observed in the fluorescence intensity from 20 to 40°C was attributed to thermal quenching of internal tryptophan fluorescence (31). Fluorescence emission scans at 20°C indicated no significant red shift in the emission maximum (data not shown) at the

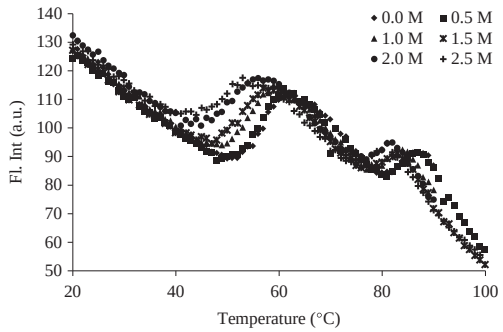

Fig. 4 Urea induced unfolding. Thermal fluorescence scans for 1.0 mg/mL MDP in the presence of urea (0 to 2.5 M).

start of the thermal ramp. Combined, this data suggested that MDP underwent two major unfolding transitions in solution.

Non-isothermal Kinetics

Non-isothermal aggregation analysis for MDP was conducting by heating MDP solutions (1.25–125 mg/mL) at 1.5°C/min. Samples collected at various time-points during the course of the experiment were analyzed for aggregated species via SEC (Fig. 5). No significant change in the monomer fraction was noted compared to the initial sample until about 50°C followed by a sudden drop in the monomer fraction for the 125 mg/mL MDP solution. Interestingly, gel formation was noted for 125 mg/mL MDP solutions above 80°C and thus aggregation data at higher temperatures could not be gathered. For solutions at lower MDP concentration (12.5 mg/mL and 1.25 mg/mL) a slower loss of monomer in the form of aggregates was noted over the time course of the experiment. For both 12.5 mg/mL and 125 mg/mL solutions, the onset of the aggregation process was ~50°C. For 1.25 mg/mL MDP, the rate was significantly slower such that the onset of any significant decrease in the monomer population could not be detected until ~75°C. Mass balance analysis indicated that nearly all the sample was accounted for in the form of monomer or soluble aggregates and no insoluble aggregates were generated during the course of the experiment for the three solutions studied. No LMW formation was noted during the experiment.

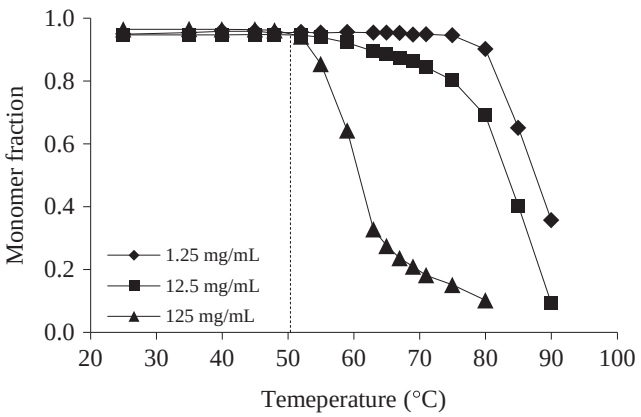

Fig. 5 Non-isothermal aggregation kinetics. Change in the monomer fraction for MDP solutions as a function of concentration with increasing temperature.

DISCUSSION

Mechanism of Aggregation

Non-native protein aggregation is assumed to be at least a two-step process; formation of the aggregation-competent non-native form of the monomer followed by or coupled to an association of this species into dimers and higher order oligomers. Either of these steps may be rate limiting for the overall process of aggregate formation. Additionally, for predictive approaches to result in any meaningful prediction of rates under refrigerated conditions, it is imperative that the rate-limiting step not change in transitioning from accelerated to long-term storage condition.

Rate-Limiting Step: Refrigerated Storage Conditions

For 1 mg/mL MDP in solution at 25°C, unfolding and refolding half-lives were determined to be in minutes (Fig. 2) which was nearly seven orders of magnitude faster compared to the rate of aggregate formation observed for 125 mg/mL MDP at 25°C (Fig. 3a). Given the technical limitations of the current biophysical techniques and the potential for simultaneous unfolding and aggregation, unfolding-refolding studies could not be conducted at 125 mg/mL MDP. It is well appreciated unfolding-refolding kinetics may potentially be altered at protein concentrations in the range of 125 mg/mL (32). However, it is improbable that an increase in concentration from 1 mg/mL to 125 mg/mL would result in a decrease in the unfolding-refolding rates by greater than seven orders of magnitude even though the unfolding-refolding half-lives may have been approximate. Additionally, reports in the literature also indicate an acceleration of the refolding step under crowded conditions (33). Thus, it could be argued that the association of the aggregation-competent form was the rate-limiting step in the aggregate formation of MDP at high protein concentrations at 25°C. Although the Gd.HCl induced unfolding and refolding studies (Fig. 2) did not specifically indicate which transition was contributing to the process under investigation, the overall unfolding-refolding kinetics for MDP were considerably faster compared to the overall rate of aggregation of MDP.

Under refrigerated storage conditions, both unfolding (significantly slower than refolding for MDP at 25°C) and association kinetics can be expected to be slower compared to 25°C.

Unfolding kinetics are known to exhibit a lower temperature dependence compared to that for the unfolding free energy change (12). Thus, it could be expected that under refrigerated conditions the overall rate of aggregate formation (related to the overall unfolding free energy change) would slow down more significantly compared to the unfolding kinetics. This would preclude the possibility of unfolding step to be the rate-determining step under refrigerated conditions. In fact, even if the unfolding step is the rate-limiting step at higher temperatures for a given protein, the association step or a step downstream of that can be expected to become the rate-limiting step under refrigerated conditions (12). Thus, the association step could be expected to be the rate-determining step for the aggregation of MDP under refrigerated storage conditions.

Rate-Limiting Step: Accelerated Storage Conditions

Initial-rate analysis was employed to determine the rate constant for MDP aggregation in solution under accelerated storage conditions. While it is well appreciated that the true order of a reaction cannot be accurately determined until the degradation has proceeded to >2–3 half-lives, higher levels of degradation are generally not-relevant to the process of formulation development. The extent of aggregation is usually limited by specifications to less than 10% and more commonly to less than 5% or even lower due to immunogenicity concerns (2,6). Thus, the initial-rate method for reaction order determination was considered to be an adequate approach for this work. The second order rate equation was rearranged in order to plot the term r_0 (Eq. 7) as a function of starting MDP concentration for the four temperatures studied (Fig. 6).

$$r_0 = \frac{1}{M_0}\left(\frac{dM}{dt}\right)_{t\to 0} = -k_1^{app} M_0 \tag{7}$$

Linear regression analysis resulted in R^2 values of 0.99, 0.99, 0.92 and 0.06 for 40°C, 35°C, 30°C and 25°C, respectively. Results indicated that for three of the four temperatures, initial loss of the monomer could be reliably described as a second order process under accelerated storage conditions. For 25°C (Fig. 6b) however, there was no meaningful relationship between the term r_0 and starting protein concentration perhaps due to the very limited extent of aggregation. Thus, the order of the reaction could not be reliably determined for 25°C. This lack of relationship highlights an inherent limitation of the initial-rate method for determining the order of a reaction when the rate of change of monomer concentration with time is small. The second order of the aggregation process (as confirmed by the data for 40°C, 35°C, 30°C) coupled with the fact that unfolding-refolding processes are first order processes indicated that association of monomers was the rate—limiting step under accelerated conditions similar to the refrigerated storage conditions.

Aggregation Prediction

Arrhenius Kinetics

Initial-rate data gathered on MDP at different temperatures (Fig. 3) was used to construct an Arrhenius plot in order to extrapolate the aggregation rate constant under refrigerated conditions and calculate the product shelf-life (Fig. 7). Extrapolation resulted in a k_1^{app} of 7.7 $X10^{-10}$ mL/(mg.day). The calculated aggregation rate constant was thus nearly two orders of magnitude smaller than the real-time (or long-term) aggregation rate constant of 8 $X10^{-8}$ mL/(mg.day) (Fig. 1). In terms of the monomer loss, the extrapolated rate constant equated to 0.003% aggregate formation per year compared to the observed rate of 0.44±0.6%/year following storage of MDP over 2 years. It is intuitive to expect that the error in the rate prediction would have been less had the accelerated aggregation rates been determined at temperatures closer to the refrigerated conditions. However, that would have been counter-productive and defeated the whole purpose of the predictive exercise. Thus, Arrhenius approximation underpredicted the aggregation rate and would have overpredicted the product shelf-life. Although, the real-time stability data most often forms the basis of determining the product shelf-life, predictive methodologies often contribute significantly to the development of product specifications. This is especially relevant when interim specifications are required prior to the long term storage stability data being available. In these cases, the predictions based on Arrhenius

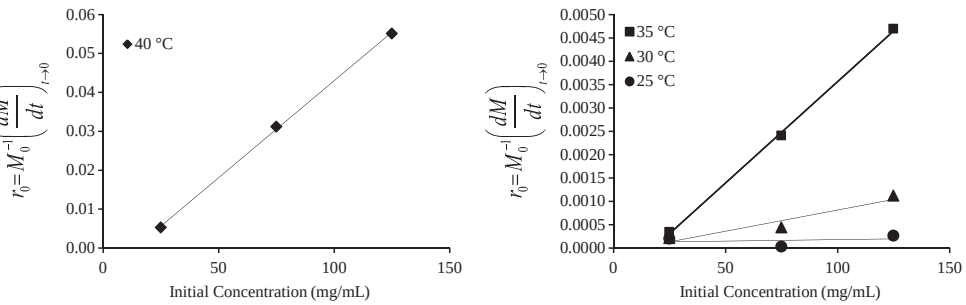

Fig. 6 Reaction order under accelerated storage conditions. Plot of the term r_0 in Eq. 7 *vs*. starting MDP concentration (M_0) for (**a**) 40°C and (**b**) 35°C, 30°C and 25°C; monomer loss was monitored for solutions with $[M_0] = 25$, 75 and 125 mg/mL.

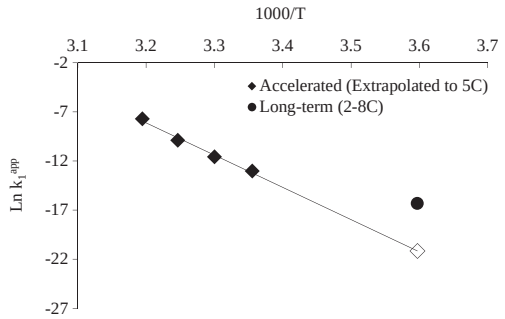

Fig. 7 Arrhenius prediction. Comparison of the aggregation rate constant extrapolated from high-temperature data using Arrhenius kinetics (*open diamond*) with the long-term (real-time) rate constant at 5°C (*closed circle*).

approach alone can lead to a significant error. For MDP, the Arrhenius prediction could have easily been used to claim a growth of for example no more than ~0.5% (an arbitrary number) in total aggregate over the course of 4–5 years. However, the product would have exhibited a 0.5% increase in total aggregate level in little over a year when refrigerated.

Extended Lumry-Eyring Model

In literature, various reasons have been cited for the non-Arrhenius behavior of protein molecules undergoing aggregation (19,20,23). Some of these include, multiple reaction steps contributing to k_1^{app}, a change in the rate-determining step with change in temperature, change in E_a with temperature, or a change in unfolding free energy with temperature i.e. the existence of a finite value for the heat capacity change for the process (enthalpy change is not constant over a broad temperature range). For MDP aggregation, it did not appear that the rate-determining step was changing from accelerated to refrigerated storage conditions (as discussed above). In an attempt to better predict the real-time aggregation rate, the unfolding process for MDP was subsequently characterized as a function of temperature in order to determine $\Delta c_{p,un}$. Two major transitions were noted in the thermal scans of MDP (Fig. 4) with onsets around ~50°C and 80°C (in absence of denaturant) indicating the unfolding of at least two domains in a non-cooperative manner. This kind of behavior is commonly observed for monoclonal antibody and Fc-fusion proteins wherein the different "constant" or conserved sequence regions may unfold separately from the antigen-binding fragment (34,35). In order to determine the transition that resulted in the generation of the aggregation-competent form of the monomer, non-isothermal studies were conducted to evaluate the impact of temperature on aggregate formation. As expected, a decrease in the soluble monomer fraction was noted with an increase in temperature for all concentrations studied. The onset temperature for the decrease in monomer fraction trended lower with increasing MDP concentration indicating the kinetic aspect of the aggregation process. The rate of aggregation increased with increasing MDP concentration, relative to the thermal ramp rate, resulting in a more significant loss of monomer at lower temperatures. Overall, the onset of the monomer loss appeared to converge around ~50°C with increasing MDP concentration consistent with the onset of the first unfolding transition (Fig. 8). These results indicated that the first transition was more relevant to the overall process of protein aggregation and was probably resulting in the generation of the aggregation-competent form of the monomer.

Equation 5 was fitted to thermal fluorescence data, gathered in presence of urea, to determine $\Delta c_{p,un}$ for MDP in solution (Fig. 9a). Not surprisingly, an effect of temperature on ΔH_m was noted indicating that, in addition to the association process, the unfolding process was also impacted by a change in solution temperature. The ΔH_m values were plotted as a function of T_m (Fig. 9b) and the $\Delta c_{p,un}$ was calculated to be 3.01 kcal/mol/°K. Using the calculated value of $\Delta c_{p,un}$ in Eq. 2 for the ELE model, the aggregation rate constant at 4°C was calculated to be 1.4 $X10^{-6}$ mL/(mg.day). The calculated rate constant was about one order of magnitude (18 times) higher than the real-time aggregation rate ($8X10^{-8}$ mL/(mg.day)). This was opposite to the prediction based on the Arrhenius approximation where the extrapolated rate constant was determined to be roughly two orders of magnitude lower (104 times) than the real-time aggregation rate. In order to understand the potential cause of the discrepancy between the real-time aggregation rate and that predicted based on ELE model, rate *versus* temperature plots were generated (Eq. 2) for a series of $\Delta c_{p,un}$ values (Fig. 10). It was noted that the precise value of the real-time rate constant could be predicted using a $\Delta c_{p,un}$ value of ~2.0 kcal/mol/°K. Regardless, although the precise value of the real-time aggregation rate could not be predicted by either model, the use of the ELE model did however (i) provide a more realistic prediction of the real-time aggregation rate and (ii) over-predicted the aggregation rate which would result in a more conservative estimate of the product shelf-life.

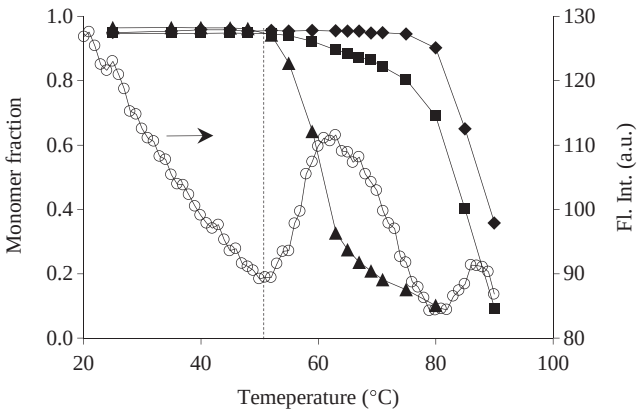

Fig. 8 Aggregation relevant transition. Comparison of fluorescence intensity for 1.0 mg/mL MDP solution (*black circles*) and monomer fraction for MDP solutions with $[M_0] = 1.25$ mg/mL (*diamond*), 12.5 mg/mL (*squares*) and 125 mg/mL (*triangles*) as a function of solution temperature.

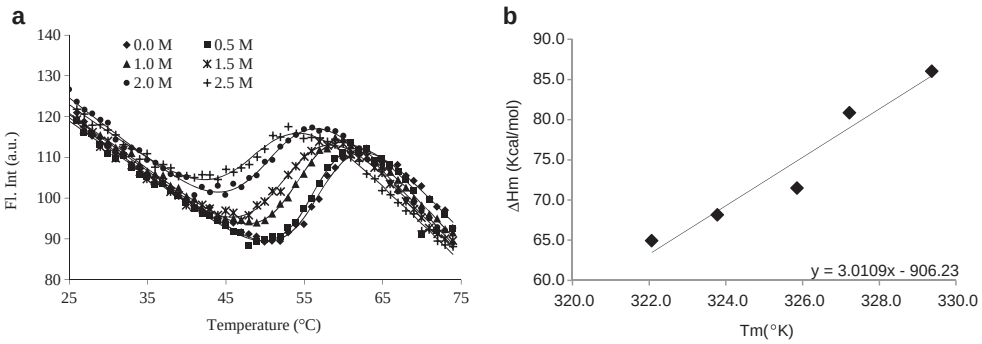

Fig. 9 Calculation of heat capacity change. (**a**) Fits of Eq. 5 to the thermal transition data (from Fig. 4) to determine T_m and ΔH_m. (**b**) Plot of ΔH_m *vs*. T_m (determined from model fitting shown in Fig. 9a).

Challenges for Aggregation Prediction of Multi-domain Proteins at High Protein Concentration

The limited capability of the currently available models for predicting the aggregation behavior of multi-domain proteins, over a pharmaceutically relevant temperature range, highlights not the irrelevance of these models but the underlying complexity of the overall aggregation process. Kayser *et al.* (21) have nicely summarized the various non-Arrhenius models (22–24,36–40), and their limitations, for predicting aggregation under refrigerated storage conditions. Most of these models are empirical or semi-empirical at best and rely on fitting the rate *vs*. temperature or percent monomer *vs*. time data with some sort of non-linear function. In doing so, these models do not offer a mechanistic basis of the overall aggregation process. In a recent work (21), authors have attempted to fit the Vogel-Tamman-Fulcher (VFT) model to the aggregation data gathered under refrigerated and accelerated conditions for five different monoclonal antibodies solutions. The results indicated that the VFT model may not be able to predict the aggregation behavior over the entire temperature range (5–40°C) studied although it did provide better fit to the data at lower temperatures. Additionally, the prediction based on the ELE model (through the calculation of $\Delta c_{p,un}$) was also unsatisfactory in terms of predicting long-term aggregation behavior. Albeit not precise in predicting long-term behavior for complex proteins, the potential advantage of the ELE models over the more empirical models lies in their mechanistic basis. The possibility that the ELE model would provide an improved mechanistic understanding of the overall aggregation process is a non trivial one and thus formed the basis of the current work.

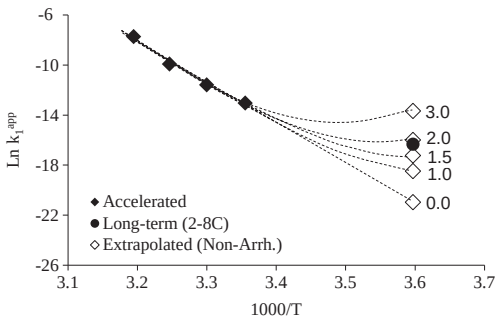

Fig. 10 Effect of heat capacity change on rate of aggregation. Plot of rate constants *vs*. inverse temperature for MDP in solution; accelerated rate constants are represented by closed diamonds and real-time/long-term rate constant by closed circle. Rate constants predicted based on the ELE (Eq. 2) are represented by open diamonds. The value next to the diamond symbols represent the $\Delta c_{p,un}$ value used to calculate the rate constant at 4°C. A $\Delta c_{p,un}$ value of 0.0 represents the linear or Arrhenius extrapolation.

Some of the key issues in predicting the aggregation rate for a multi-domain protein like MDP at high protein concentrations, compared to two-state proteins like bG-CSF are (i) the complexity of the unfolding process and the difficulty in detecting the aggregation-competent form, (ii) the potential for interactions between the multiple transition states or domains of the protein (iii) available biophysical methods not being conducive to working at high protein concentrations (iv) the change in activity or effective concentration of the protein due to intermolecular interactions i.e. solution non-ideality etc. In our studies, we noted two distinct major transitions for MDP at 1 mg/mL (TSIF) and attributed the generation of the aggregation-competent form to the first transition (T_{Onset} = ~50°C) based on non-isothermal kinetics data. However, it is quite plausible that certain minor transition(s) that precede the first detectable transition could be responsible for the generation of the aggregation-competent form of the monomer. These states, commonly referred to as molten globule or partially unfolded states, have been known to be directly involved in protein aggregation (41,42). For proteins, it is quite possible for these molten globule states to have a $\Delta c_{p,un}$ value lower than that of the first complete transition detected via biophysical techniques (43). A closer look at the TSIF unfolding data hinted at the possibility of the presence of molten globule like states for MDP (Fig. 11). The TSIF data exhibited a curvature, albeit relatively minor, in the pre-transition region of the thermal scan possibly hinting towards the existence of molten globule or partially unfolded states of MDP (44). Inter-domain interactions, which can potentially exist and affect the unfolding/refolding behavior, can also interfere with the identification of the unique transition that results in generation of the aggregation-competent species. Another aspect that needs to be noted is the potential for

simultaneous aggregation to some extent as unfolding progresses in heat-induced unfolding experiments (45). Based on the results of the unfolding studies at 1 mg/mL (Fig. 4) and non-isothermal kinetics study at 1.25 mg/mL (Fig. 5) for temperatures at least up to ~ 50°C, any significant level of simultaneous aggregation and unfolding could be ruled out in the absence of the denaturant (most of the protein is retained as the monomer fraction as temperature is ramped up to ~ 50°C). However, that may not be true for MDP solutions in the presence of the denaturant; the extent of aggregation as unfolding progresses may be enough to interfere with the absolute measurement of $\Delta c_{p,un}$. This may introduce some level of error in the $\Delta c_{p,un}$ measurement making it somewhat apparent rather than absolute measure of the thermodynamics of unfolding.

Additionally, the aggregation studies and unfolding studies for $\Delta c_{p,un}$ calculation were conducted in two quite distinct concentration regimes (1.0 mg/mL for unfolding *vs.* 125 mg/mL for aggregation). Limited unfolding studies conducted at 125 mg/mL (via TSEF) also hinted at the possibility of certain transitions not being fully captured via TSIF studies. Thermal fluorescence scans generated at 125 mg/mL via TSEF exhibited an onset of transition at ~35°C nearly 15°C less than that observed during TSIF studies (~50°C). However, $\Delta c_{p,un}$ determination could not be conducted at 125 mg/mL since individual transitions could not be resolved via TSEF studies. There were other challenges in conducting denaturant-induced unfolding studies at high MDP concentration. Firstly, the possibility of concurrent aggregation and unfolding processes erroneously impacting the determination of $\Delta c_{p,un}$ could not be precluded at 125 mg/mL. Secondly, the presence of denaturant and heat stress at high protein concentrations could have potentially resulted in lowering of the gelation temperature (below 80°C) further complicating the interpretation of the protein unfolding data. As a result of these limitations, unfolding studies and the determination of $\Delta c_{p,un}$ could not be conducted at 125 mg/mL.

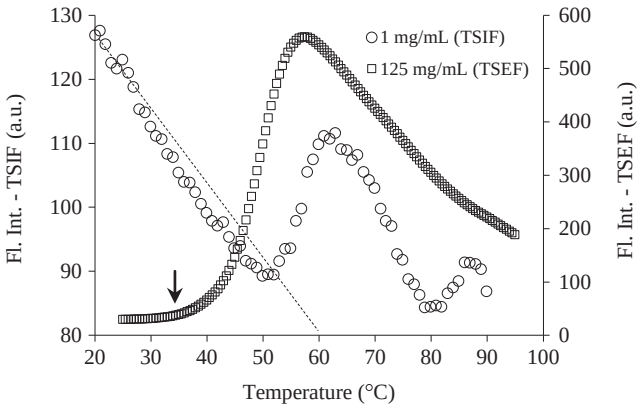

Fig. 11 Unfolding transitions as a function of MDP concentration. Comparison between TSIF (1.0 mg/mL MDP) and TSEF (125 mg/mL MDP) data for MDP in solution in absence of urea.

In addition to the technical challenges in identifying and characterizing the aggregation-competent form and working at high protein concentrations, another challenge for accurate rate prediction via the non-Arrhenius approach stems from the exponential dependence of aggregation rate on $\Delta c_{p,un}$ (Eq. 2). For example, during unfolding studies of MDP an error of ~5% was noted in the measured values of the $\Delta c_{p,un}$. In terms of aggregation rate, this error in $\Delta c_{p,un}$ equates to an error of ~45% in the predicted rate constant. Thus, it is all the more necessary to not only attempt to identify the aggregation-relevant transition but also to accurately determine the value of $\Delta c_{p,un}$ for improving the overall rate prediction. Regardless of the limitations discussed above, it can be safely assumed that that the possibility of the more aggregation relevant transition, which is relatively minor and more or less undetectable, having a $\Delta c_{p,un}$ value higher than that of the first detected transition is quite minimal. That being the case, the rate prediction based on the ELE model, if not completely accurate, would always result in a more conservative estimate of the product shelf-life.

SUMMARY

The work presented here highlights the significance of incorporating unfolding thermodynamics for aggregation rate, and subsequently the shelf-life prediction of a multi-domain protein in solution. In the absence of better predictive models, it is quite tempting to employ the simplistic Arrhenius extrapolation to protein aggregation. However, as shown here, the Arrhenius approach can be misleading and result in overly liberal estimates of the product shelf-life. The ELE approach does provide a potential path for a more accurate and conservative estimation of the product shelf-life. While the prediction of the precise aggregation rate during protein product development is often required, it is not the only goal of employing predictive methodologies. Quite often an understanding of the potential upper and lower limits of aggregation is also required. This may be for the purpose of developing product specifications with respect to protein aggregates either during interim product development or during long-term stability studies. In these instances, a predictive methodology combining the Arrhenius and the ELE approximations can be successfully leveraged to better understand the lower and upper limits of aggregation rate i.e. best and the worst-case scenarios with respect to the aggregation potential of the product. This bracketing approach can also be beneficial when multiple attributes like solution viscosity and aggregation (often oppositely impacted by ions for example) need to be optimized simultaneously. Worst-case estimates of protein aggregation can be established for a formulation preferred for its viscosity attribute or vice-versa. Obviously, it is of utmost significance that the constancy of the mechanism of reaction (order of reaction, rate-limiting step etc.) over the course of the

entire temperature range (stress as well as refrigerated) be ascertained first. This work also highlights some of the challenges of working with high concentrations of multi-domain proteins that do not follow a simple two-state transition. However, the impact of these challenges on rate prediction, while not completely mitigated, can be minimized by employing orthogonal techniques to better understand and characterize the overall conformational and assembly processes of a given protein in solution.

REFERENCES

1. Fradkin AH, Carpenter JF, Randolph TW. Immunogenicity of aggregates of recombinant human growth hormone in mouse models. J Pharm Sci. 2009;98:3247–64.
2. Rosenberg AS. Effects of protein aggregates: an immunologic perspective. AAPS J. 2006;8:E501–7.
3. Moore WV. The role of aggregated hGH in therapy of hGH-deficient children. J Clin Endocrinol Metab. 1978;46:20–7.
4. Mooreand WV, Leppert P. Role of aggregated human growth hormone (hGH) in development of antibodies to hGH. J Clin Endocrinol Metab. 1980;51:691–7.
5. Rosenberg AS. Effects of protein aggregates: an immunologic perspective. AAPS Journal. 8:Article 59: (http://www.aaps.org) (2006).
6. Schellekens H. The immunogenicity of therapeutic proteins. Discov Med. 2010;9:560–4.
7. Brinks V, Jiskoot W, Schellekens H. Immunogenicity of therapeutic proteins: the use of animal models. Pharm Res. 2011;28:2379–85.
8. Casadevall N, Nataf J, Viron B, *et al*. Pure red-cell aplasia and antierythropoietin antibodies in patients treated with recombinant erythropoietin. N Engl J Med. 2002;346:469–75.
9. Li J, Yang C, Xia Y, *et al*. Thrombocytopenia caused by the development of antibodies to thrombopoietin. Blood. 2001;98:3241–8.
10. Zwickl CM, Cocke KS, Tamura RN, *et al*. Comparison of the immunogenicity of recombinant and pituitary human growth hormone in rhesus monkeys. Fundam Appl Toxicol. 1991;16:275–87.
11. FDA. Meeting of the biological response modifiers advisory committee, *Center for Biologics Evaluation and Research*, Bethesda MD., July 15, 1999.
12. Weiss WF, Young TM, Roberts CJ. Principles, approaches, and challenges for predicting protein aggregation rates and shelf life. J Pharm Sci. 2009;98:1246–77.
13. Mahler HC, Friess W, Grauschopf U, *et al*. Protein aggregation: pathways, induction factors and analysis. J Pharm Sci. 2009;98:2909–34.
14. Liu J, Nguyen MDH, Andya JD, *et al*. Reversible self-association increases the viscosity of a concentrated monoclonal antibody in aqueous solution. J Pharm Sci. 2005;94:1928–40.
15. Fesinmeyer RM, Hogan S, Saluja A, *et al*. Effect of ions on agitation- and temperature-induced aggregation reactions of antibodies. Pharm Res. 2009;26:903–13.
16. Kendrick BS, Li T, Chang BS. Physical stabilization of proteins in aqueous solutions. In: Carpenterand JF, Manning MC, editors. Rational design of stable protein formulations: Theory and practice, vol. 13. New York: Kluwer Acaddmic/Plenum; 2002. p. 203.
17. Lumryand R, Eyring H. Conformation changes of proteins. J Phys Chem. 1954;58:110–20.
18. Roberts CJ. Non-native protein aggregation kinetics. Biotechnol Bioeng. 2007;98:927–38.
19. Roberts CJ, Darrington RT, Whitley MB. Irreversible aggregation of recombinant bovine granulocyte-colony stimulating factor (bG-CSF) and implications for predicting protein shelf life. J Pharm Sci. 2003;92:1095–111.
20. Wangand W, Roberts CJ. Non-Arrhenius protein aggregation. AAPS J. 2013;15:840–51.
21. Kayser V, Chennamsetty N, Voynov V, *et al*. Evaluation of a non-Arrhenius model for therapeutic monoclonal antibody aggregation. J Pharm Sci. 2011;100:2526–42.
22. Magari RT, Murphy KP, Fernandez T. Accelerated stability model for predicting shelf-life. J Clin Lab Anal. 2002;16:221–6.
23. Matagne A, Jamin M, Chung EW, *et al*. Thermal unfolding of an intermediate is associated with non-Arrhenius kinetics in the folding of hen lysozyme. J Mol Biol. 2000;297:193–210.
24. Roberts CJ. Kinetics of irreversible protein aggregation: analysis of extended lumry-eyring models and implications for predicting protein shelf life. J Phys Chem B. 2003;107:1194–207.
25. Liand Y, Roberts CJ. Lumry-Eyring nucleated-polymerization model of protein aggregation kinetics. 2. Competing growth via condensation and chain polymerization. J Phys Chem B. 2009;113:7020–32.
26. Andrewsand JM, Roberts CJ. A Lumry-Eyring nucleated polymerization model of protein aggregation kinetics: 1. Aggregation with pre-equilibrated unfolding. J Phys Chem B. 2007;111:7897–913.
27. Bolenand DW, Santoro MM. Unfolding free energy changes determined by the linear extrapolation method. 2. Incorporation of delta G degrees N-U values in a thermodynamic cycle. Biochemistry. 1988;27:8069–74.
28. Pace CN, Hebert EJ, Shaw KL, *et al*. Conformational stability and thermodynamics of folding of ribonucleases Sa, Sa2 and Sa3. J Mol Biol. 1998;279:271–86.
29. Scottand KA, Clarke J. Spectrin R16: broad energy barrier or sequential transition states? Protein Sci. 2005;14:1617–29.
30. Oliveberg M, Tan YJ, Silow M, *et al*. The changing nature of the protein folding transition state: implications for the shape of the free-energy profile for folding. J Mol Biol. 1998;277:933–43.
31. Lakowicz JR. Principles of frequency-domain fluorescence spectroscopy and applications to cell membranes. Subcell Biochem. 1988;13:89–126.
32. van den Berg B, Wain R, Dobson CM, *et al*. Macromolecular crowding perturbs protein refolding kinetics: implications for folding inside the cell. EMBO J. 2000;19:3870–5.
33. Du F, Zhou Z, Mo ZY, *et al*. Mixed macromolecular crowding accelerates the refolding of rabbit muscle creatine kinase: implications for protein folding in physiological environments. J Mol Biol. 2006;364:469–82.
34. Ionescu RM, Vlasak J, Price C, *et al*. Contribution of variable domains to the stability of humanized IgG1 monoclonal antibodies. J Pharm Sci. 2008;97:1414–26.
35. Vermeerand AW, Norde W. The thermal stability of immunoglobulin: unfolding and aggregation of a multi-domain protein. Biophys J. 2000;78:394–404.
36. Tolgyesi F, Ullrich B, Fidy J. Tryptophan phosphorescence signals characteristic changes in protein dynamics at physiological temperatures. Biochim Biophys Acta. 1999;1435:1–6.
37. King SY, Kung MS, Fung HL. Statistical prediction of drug stability based on nonlinear parameter estimation. J Pharm Sci. 1984;73:657–62.
38. Fulcher GS. Analysis of recent measurements of the viscosity of glasses. J Am Ceram Soc. 1925;8:339–55.
39. Duggleby RG. Regression analysis of nonlinear Arrhenius plots: an empirical model and a computer program. Comput Biol Med. 1984;14:447–55.
40. Roberts C. Nonnative protein aggregation. Springer New York: Misbehaving Proteins; 2006. p. 17–46.
41. McParland VJ, Kad NM, Kalverda AP, *et al*. Partially unfolded states of beta(2)-microglobulin and amyloid formation in vitro. Biochemistry. 2000;39:8735–46.

42. Kim YS, Randolph TW, Manning MC, *et al*. Congo red populates partially unfolded states of an amyloidogenic protein to enhance aggregation and amyloid fibril formation. J Biol Chem. 2003;278: 10842–50.
43. Roberts CJ, Das TK, Sahin E. Predicting solution aggregation rates for therapeutic proteins: approaches and challenges. Int J Pharm. 2011;418:318–33.
44. Sharmaand VK, Kalonia DS. Temperature- and pH-Induced multiple partially unfolded states of recombinant human interferon-a2a: possible implications in protein stability. Pharm Res. 2003;20: 1721–9.
45. Brummitt RK, Nesta DP, Roberts CJ. Predicting accelerated aggregation rates for monoclonal antibody formulations, and challenges for low-temperature predictions. J Pharm Sci (2011).